JCTC Journal of Chemical Theory and Computation

Influence of Adsorbate-Free Atoms on Δ-XANES Signatures

Stanislav Stoupin*

Department of Chemistry and Chemical Biology, Northeastern University, Boston, Massachusetts 02115

Received December 8, 2008

Abstract: The use of differential X-ray Absorption Near Edge Spectroscopy (Δ-XANES) for analysis of site specific adsorption on metallic electrodes relies on theoretical Δ-XANES signatures for analysis of experimental Δ-XANES fingerprints. A simple model, currently used in the analysis, considers changes in X-ray absorption properties of adsorbing atoms only. This model has been extended to include changes in X-ray absorption for other atoms of the same type that remain adsorbate-free. Configurational averaging has been applied to calculate difference spectra of a Pt_6 cluster with an oxygen atom adsorbed at different sites. The extended theory shows that contribution of the adsorbate-free atoms might become significant as it affects the shape profiles of the theoretical signatures. The effect, most prominent at the absorption edge energy, is interpreted in terms of change in the electronic structure of the cluster due to oxygen adsorption. In addition to model dependence of the theoretical signatures, challenges to the application of Δ-XANES to the experimentally obtained fingerprints are discussed.

Introduction

Knowledge of adsorbate binding sites is essential for understanding catalytic and electrochemical reactions. For instance, oxygen adsorption on a complex surface of a high dispersion Pt based catalyst is an elementary step in both anode and cathode fuel cell reactions. Oxygen participation in these reactions depends on a large number of parameters including electrode potentials, adsorbate content, catalyst composition, and morphology. This situation alone generates high demand for reliable methods of surface adsorbate analysis under reaction conditions. Numerous studies report systems and conditions where a particular type of catalyst-adsorbate interaction prevails. However, only a few in situ methods provide structural and/or electronic information from which details of adsorbate-catalyst interaction can be inferred. X-ray Absorption Spectroscopy (XAS) is one of the most valuable techniques that serve the purpose.[1] XAS at the Pt L_3 X-ray absorption edge is widely used for in situ characterization of Pt-based catalysts.[2−14]

* Corresponding author e-mail: sstoupin@aps.anl.gov. Current address: Advanced Photon Source, Argonne National Laboratory, IL 60439.

An emerging strategy for the analysis of site-specific adsorption is differential X-ray Absorption Near Edge Spectroscopy (Δ-XANES).[8−14] XANES of a catalyst under adsorbate-free conditions is subtracted from XANES under conditions conducive to adsorption (e.g., by altering the potential or chemical environment). The Δ-XANES is sensitive to changes in metal-adsorbate and metal−metal interactions. The interpretation of the experimental Δ-XANES ($\Delta\mu$-fingerprint) is at an early stage of development. Ramaker et al. calculate theoretical XANES of model clusters (e.g., Pt_6 Janin cluster[15]) with and without adsorbates using a full-multiple scattering code (FEFF8), which employs self-consistent field calculations of the local electronic structure.[16,17] The corresponding theoretical Δ-XANES, hereafter referred to as $\Delta\mu$-signatures, are used for analysis of $\Delta\mu$-fingerprints.[8−14] The $\Delta\mu$-fingerprints are correlated to adsorbate coverage profiles by plotting magnitudes of certain characteristic peaks versus parameters of interest (e.g., electrode potential, adsorbate concentration).

To date, the $\Delta\mu$-signatures for oxygen adsorption in the four oxygen-adsorption configurations only include X-ray absorption events from a single adsorbing Pt atom (atom-0 in Figure 1) of the Janin cluster at the Pt L_3 edge.[9] Further, these will be referred to as *limited-adsorber* $\Delta\mu$-signatures.

10.1021/ct800544a CCC: $40.75
Published on Web 04/02/2009

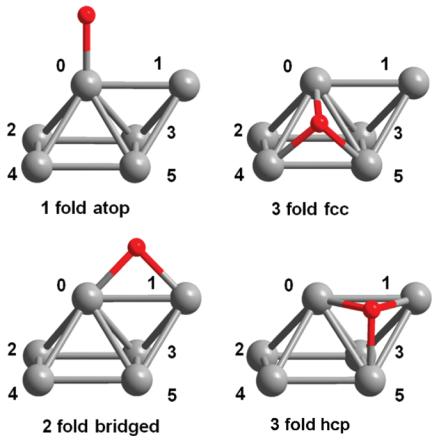

Figure 1. Oxygen adsorption configurations of the Janin Pt_6 cluster and numbering of the Pt atoms.

Analysis of experimental fingerprints using the *limited-adsorber* signatures is based on an assumption that the presence of adsorbate does not alter X-ray absorption properties of the adsorbate-free atoms of an electrochemical system under consideration. This assumption seems to be applicable in the case of low adsorbate coverage where a small number of adsorbed species does not significantly disturb the electronic structure of the system. However, it is not obvious in a case where the number of adsorbed species is comparable to the number of atoms in the catalytic nanoparticle.

For example, Ankudinov et al.[18] showed that changes in the near-neighbor Pt scattering potentials due to adsorbate-Pt interaction (i.e., changes in the Pt electronic structure) may dominate over the effect of Pt-adsorbate photoelectron multiple scattering. Furthermore, Bazin et al. discuss the importance of configurational averaging when calculating XANES of small clusters.[19] It was illustrated that per-atom Pt L_3 edge XANES differ among nonequivalent Pt sites. In this regard, presence of a single adsorbate on the six-atom Pt Janin cluster can be considered as a case of intermediate coverage.

Because XAS probes all cluster atoms, a more rigorous theoretical treatment of Δ-XANES requires inclusion of X-ray absorption events originating from all cluster atoms (i.e., *all-atoms* model). In this work, electronic properties of the Janin cluster in the four oxygen-adsorption configurations are correlated to the shape profiles of atom specific $\Delta\mu$-signatures based on results of FEFF8 calculations. It is shown that the shape profiles of *all-atoms* $\Delta\mu$-signatures differ from the *limited-adsorber* $\Delta\mu$-signatures currently used for Δ-XANES analysis of oxygen adsorption. Limitations on the applicability of both models are discussed.

Computational Approach

The Pt L_3 XANES white-line is a strong peak due to unoccupied Pt d-densities of states (d-DOS) near the photoelectron threshold energy (i.e., Fermi level). The FEFF8 code default Hedin-Lundqvist self-energy (omitted EXCHANGE card) adequately reproduces the Pt white-line.[20−23] The final states calculated without the presence of a screened core-hole (NOHOLE card) show better agreement with experimental data.[22−24] An atomic potential (IPOT) was assigned to the adsorbed oxygen and every Pt atom of the Janin cluster. Thus, the number of unique atomic potentials in each calculation was 6 for the adsorbate-free (clean) cluster and 7 for the clusters with adsorbed oxygen. It is noted that the number of unique potentials can be reduced for the clean, 1-fold atop and 2-fold bridged configurations due to their symmetry.

The version of the code used in this work was FEFF8.4. The Pt L_3 XANES spectrum was calculated for each Pt atom by assignment of the X-ray absorber atomic potential (IPOT 0) to that atom. This procedure was applied to all configurations of the Janin cluster using the four oxygen adsorption sites as previously reported (Figure 1). The signatures were computed on a per-atom basis using Athena program.[25] The absorption edge energy (11564 eV) was assigned to the inflection point of the calculated XANES for atom-0 of the adsorbate-free cluster, which resulted in 2.6 eV shift of the FEFF8 absolute energy scale. Thus, the code underestimates the absolute edge energy if defined as the inflection point. The shift was applied to all calculated spectra.

Results

The white-line intensities for atom-0 increase in any of the four oxygen-adsorption configurations, which is accompanied by reduction in the population of the atom-0 d-states (Figure 2a). The subtraction of the atom-0 clean cluster spectrum from the atom-0 atop or n-fold adsorption configurations yields the *limited-adsorber* signatures with no derivative-like appearance (i.e., signatures of Ramaker et al.[9−11] reproduced in our calculations). In contrast, only a minor change in the population of the d-states occurs for the adsorbate-free atoms. For these atoms, the variation in the white-line intensity with oxygen-adsorption configuration is small relative to that of any of the adsorbing atoms. Figure 2b shows XANES of the clean cluster atom-2 and that of the atom-2 in the 3-fold fcc configuration. The shift to higher energy of the 3-fold XANES results in the derivative-like appearance of the atom-2 $\Delta\mu$-signature (inset in Figure 2b).

The shape of the XANES relates to FEFF8 calculated Pt local d-DOS (d-LDOS) spectra above the Fermi level. Figure 2c contrasts d-LDOS of atom-0 in the clean cluster (blue line) with that of the atom-0 in the atop configuration (red line). Although the number of vacant states of the atop atom-0 is higher just above the Fermi level, the density of states reduces at higher energies and becomes lower than that of atom-0 in the clean cluster. This reduction is correlated with intensity of XANES of the atom-0 (Figure 2a). Similarly, the variation of d-LDOS of atom-2 in the 3-fold fcc configuration (Figure 2d − purple line) vs d-LDOS of atom-2 of the clean cluster (blue line) is correlated with the shapes of atom-2 XANES (Figure 2b). In general, for every Pt atom in the clusters, self-consistent field calculations of the local electronic structure yield variation of d-LDOS spectra upon oxygen adsorption. These variations correlate with the shape and intensity of the calculated atom-specific XANES/Δ-XANES and are rather significant for adsorbate-free atoms of the Janin cluster.

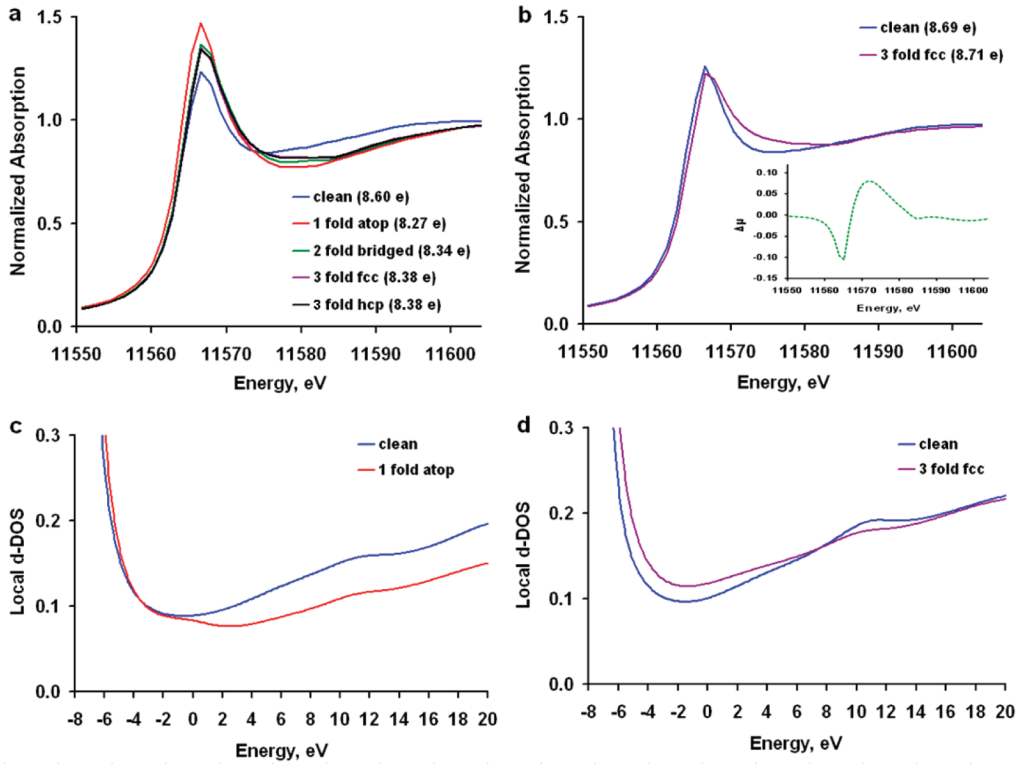

Figure 2. Variation of the calculated atom specific Pt L_3 edge XANES and d-LDOS with oxygen adsorption configuration: (a) XANES of adsorbing atom-0: the dominant variation is the increase in the white-line intensity with reduction in the population of the d states (the populations are shown in the legend). (b) XANES of adsorbate-free atom-2 in the 3-fold fcc configuration (purple) and of atom-2 in the clean cluster (blue). The inset shows the result of subtractive normalization of the purple line to the blue line (i.e., atom-2 $\Delta\mu$-signature in the 3-fold fcc configuration). (c) d-LDOS of atom-0 in the atop configuration (red) and of atom-0 in the clean cluster (blue). (d) d-LDOS of adsorbate-free atom-2 in the 3-fold fcc configuration (purple) and of atom-2 in the clean cluster (blue).

Figure 3a-d summarizes the $\Delta\mu$-signatures on a per-atom basis in all configurations. The blue lines are the average of the per-atom signatures (*all-atoms* $\Delta\mu$-signatures) for each of the adsorption configurations. Averaging is for illustrative purposes to mimic the Δ-XANES fingerprint of the Janin cluster as if it was a real adsorption system (i.e., all Pt atoms are equally probed by the X-rays). With the exception of the 1-fold atop configuration, the *all-atoms* $\Delta\mu$-signatures have a derivative-like appearance. The red lines (Figure 3a-d) are the *limited-absorber* $\Delta\mu$-signatures based on X-ray absorption events originating only from one adsorbing atom (atom-0). The shape profiles and intensities of the *all-atoms* $\Delta\mu$-signatures (blue lines) are compared to the respective *limited-adsorber* signatures (red lines) (Figure 3a-d). FEFF8 calculated charge transfer magnitudes, d-LDOS populations (on a per-atom basis), and Fermi levels of the clean cluster, the 1-fold atop, and the n-fold cluster configurations are summarized in Table 1.

Discussion

The factors that determine the shape and intensity of the atom-specific signatures at low energy side (i.e., in vicinity of the absorption edge) are variations in the white-line intensity and changes in the absorption edge energy. As noted earlier, the primary factor for adsorbing atoms is the increase in the white-line intensity correlated to the reduction in the population of the d-LDOS due to charge transfer effects (e.g., atom-0 - Figure 2a). In the following discussion, the influence of changes in the absorption edge energy is analyzed.

Fermi level of any given cluster sets the photoelectron threshold for all atoms in that cluster (Table 1). With the exception of the 1-fold atop configuration, the Fermi level shifts positively for all other clusters with an adsorbed oxygen atom (n-fold configurations). Thus, a positive shift of the absorption edge, leading to a derivative-like appearance, is expected for every Pt atom in the n-fold configurations. Although the direction of this shift is correlated with the shift of the Fermi level, it is noted that the absolute energy of the absorption edge is an estimate. The code estimates absolute energies by calculating the difference in the total relativistic Dirac/Fock energy of an atom with and without a core-hole. Under an assumption that the absolute energies are equally underestimated for all atoms, the shift of the absorption edge energy is due to the shift in the Fermi level.

The loss of intensity at the edge region due to the positive shift of the absorption edge is compensated by an increase in the white-line intensity upon adsorption of oxygen. This compensation can be complete (e.g., $\Delta\mu$ of atom-0 in all n-fold configurations − Figure 3a-d) or incomplete, such that a small negative peak is still present (e.g., $\Delta\mu$ of atom-4 and atom-5 in Figure 3b). In contrast, the negative peak at the low energy side is substantial in the adsorbate-free atom signatures because the loss of intensity due to the absorption edge shift is not countered by an increase in the white-line

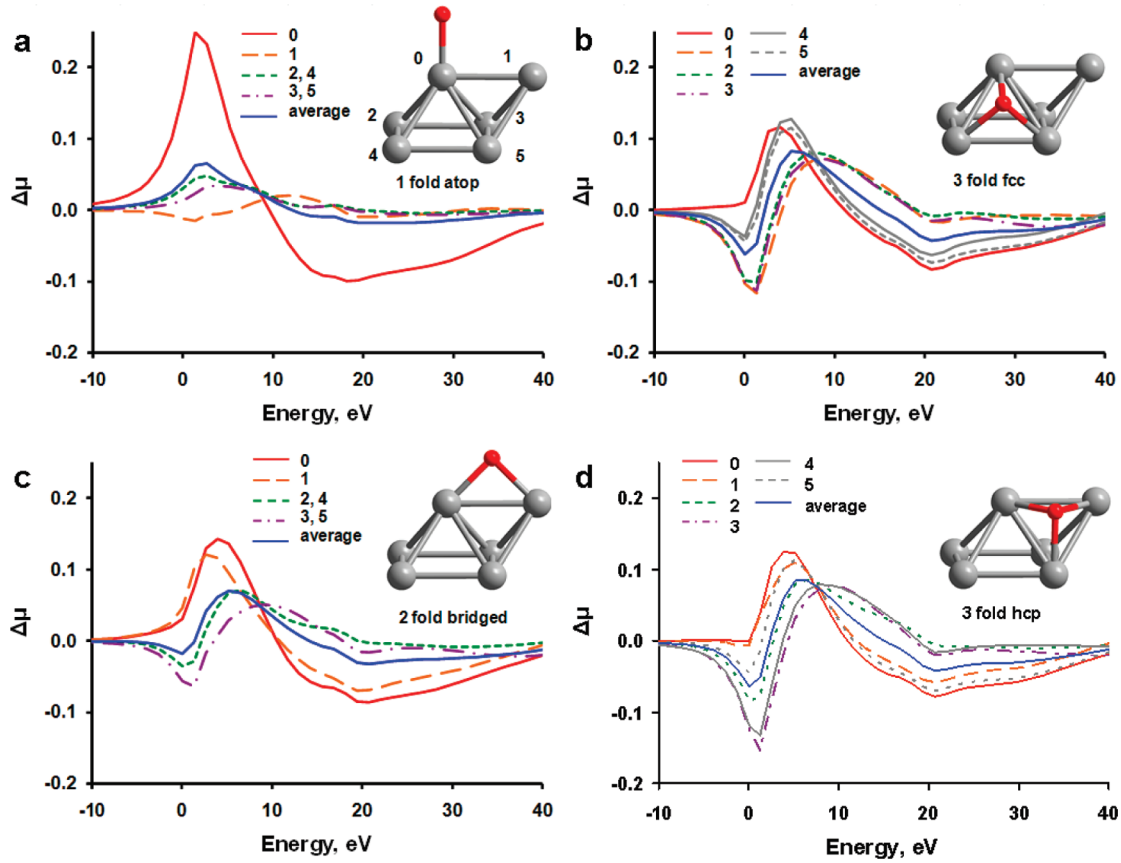

Figure 3. FEFF8 $\Delta\mu$ signatures on a per-atom basis calculated for Pt_6 Janin cluster with O adsorbed on the (a) 1-fold atop, (b) 3-fold fcc, (c) 2-fold bridged, and (d) 3-fold hcp sites. The red lines are signatures of Ramaker et al. reproduced in our calculations (*limited-adsorber* signatures). The blue lines are the average value $\Delta\mu$-signatures (*all-atoms* signatures).

Table 1. FEFF8 Atomic Partial Charge in Units of the Elementary Charge, Atomic d Electron Counts, and Cluster Fermi Levels

atom/cluster	clean	1-fold atop	2-fold bridged	3-fold fcc	3-fold hcp
O	–	−0.246	−0.095	0.012	0.006
Pt0	0.051(8.60)	0.320(8.27)[a]	0.262(8.34)[a]	0.239(8.38)[a]	0.223(8.38)[a]
Pt1	−0.030(8.70)	−0.022(8.70)	0.239(8.41)[a]	−0.232(8.72)	0.167(8.43)[a]
Pt2	−0.033(8.69)	−0.044(8.67)	−0.133(8.69)	−0.240(8.71)	−0.225(8.70)
Pt3	0.023(8.62)	0.018(8.62)	−0.070(8.64)	−0.158(8.65)	−0.154(8.68)
Pt4	−0.033(8.69)	−0.044(8.67)	−0.133(8.69)	0.171(8.44)[a]	−0.223(8.73)
Pt5	0.023(8.62)	0.018(8.62)	−0.070(8.64)	0.208(8.42)[a]	0.207(8.42)[a]
E_F	−7.135	−7.198	−7.021	−6.830	−6.816

[a] Adsorbing Pt atoms.

intensity. Thus, the derivative-like appearance of the n-fold *all-atoms* signatures of the Janin cluster is characteristic to its adsorbate-free atoms.

An important remark is that the offered interpretation of the derivative-like shape is not applicable to the case of hydrogen adsorption on Pt. The effect of H adsorption on Pt L_3 edge XANES has been extensively studied.[8,18,26] A substantial negative contribution was observed experimentally and modeled by *limited-adsorber* signatures for H in the n-fold configurations. In order to validate the *all-atoms* model, the per-atom $\Delta\mu$-signatures were calculated for H atom adsorbed on the Janin cluster in the four configurations. The results are presented in the Supporting Information. In contrast to the case of O, the shifts of the Fermi level and the charge transfer effects are insufficient to explain the negative contribution. The resulting $\Delta\mu$-signatures of the adsorbate-free atoms of the n-fold configurations are similar to the n-fold *limited-adsorbate* signature reported earlier. Thus, in the case of hydrogen, configurational averaging does not produce new features in the spectral shape of the theoretical Δ-XANES.

If considered as theoretical standards, the calculated $\Delta\mu$-signatures of the adsorbate-free atoms are likely exaggerated due to the small size of the cluster. For example, realistic electrochemical Pt/C clusters are usually about 1.5−2 nm in size (100−300 atoms assuming spherical shape). Available Δ-XANES fingerprints for O and OH adsorption on such Pt/C materials indicate the presence of negative contribution to the edge region at high adsorbate coverages.[9,11] The effect has been attributed to increased Pt−O coordination due to the presence of subsurface oxygen at higher electrode potentials. The *all-atoms* model suggests that the effect is

caused by the change in absorption properties of adsorbate-free atoms due to a shift in the Fermi level. A greater shift is expected in the case of high coverage, while only minimal changes occur in local electronic structure for atoms that do not participate in bonding with oxygen. Due to a large number of such atoms in the realistic electrochemical cluster, the individual derivative-like $\Delta\mu$-signatures may constructively interfere with each other, which would result in the experimentally observed negative contribution.

In order to minimize the influence of the adsorbate-free atoms at the edge energy, an alignment of Fermi levels can be performed prior to subtraction of XANES if additional information about the shift is extracted from experiment data. This approach has been implemented for supported Pt catalysts in gas phase systems.[26,27] The number of Pt atoms in the supported clusters of the gas phase catalysts is comparable to the number of atoms in the Janin cluster. Thus, careful alignment procedure is of particular importance for these small clusters. Pt L_2 edge XANES of the samples with and without adsorbates were aligned under an assumption that the onset of the absorption edge is not affected by the presence of adsorbates. The Pt L_3 edge XANES were aligned relative to the L_2 edges using Extended X-ray Absorption Fine Structure (EXAFS). EXAFS refers to small oscillations in the X-ray absorption coefficient at 40−50 eV above the edge energy, which contain local structural information. The L_3 and L_2 EXAFS spectra are equivalent for the same sample under the same experimental conditions.

Unfortunately, any alignment procedure contains an uncertainty, which might lead to misinterpretation of the experimental fingerprints. Reliability of the fingerprints at the low energy side is questionable because subtraction of XANES at these energies is most sensitive to the alignment errors. The energy scale of a conventional X-ray absorption experiment is defined by mechanical motion of an X-ray double crystal monochromator. The scale slightly fluctuates from one energy scan to another. If alignment of experimental spectra produces an error ΔE, the threshold level that sets the lowest reliable magnitude of $\Delta\mu$ can be derived as follows.

The absorption coefficient is a weak function of electrochemical environment. For the purpose of error estimation, one can assume that it is only a function of X-ray energy E. A difference between two misaligned spectra of a certain representative X-ray absorption standard with absorption coefficient $\mu(E)$

$$\Delta\mu(E, \Delta E) = \mu(E + \Delta E) - \mu(E) \quad (1)$$

can be expressed through the derivative of the absorption coefficient in a vicinity of a certain energy E_0

$$\Delta\mu(E_0, \Delta E) \approx \frac{d\mu}{dE}(E_0)\Delta E \quad (2)$$

A threshold reliability level in $\Delta\mu$ can be estimated using eq 2 for any given energy. The absorption edge energy is often assigned to the inflection point. Hence, the lowest reliable $\Delta\mu$ at the absorption edge is defined by the maximum of the derivative. For Pt L_3 edge XANES this value is about 0.3 eV^{-1}. The alignment error ΔE is affected by a number of factors such as quality of reference data used for alignment, the alignment algorithm, intrinsic broadening of X-ray absorption spectra due to finite core-hole lifetime, and instrumental resolution. A reasonable estimate of $\Delta E = 0.1$ eV is on the order of a step size of a fine energy grid for XANES data collection and about 10 times less than a spectral bandpass of a conventional double crystal X-ray monochromator. This sets a reliability threshold level of $\Delta\mu = 0.03$ at the Pt L_3 edge.

Unfortunately, the threshold level is on the same order of magnitude as the experimentally observed negative contributions to Δ-XANES fingerprints at the absorption energy edge. In order to minimize the drift of the energy scale, alternative methods for obtaining Δ-XANES fingerprints are required. One of the alternatives is to utilize an energy dispersive X-ray absorption spectrometer.[3,5,28,29] Such an instrument has no moving components and enables measurements of X-ray absorption spectra with minimal energy drift. In particular, this approach has enabled observation of femtometre-scale atomic displacements by difference EXAFS.[29] Although, a higher noise level (i.e., lower sensitivity) is expected in comparison to traditional XAS (energy scans), successful applications of the dispersive method to electrochemical systems have been reported.[3,5,30] In-situ EXAFS spectra were recorded and quantitatively analyzed. EXAFS is a weak effect in comparison to XANES. This suggests applicability of the dispersive method to Δ-XANES. It is expected that minimization of energy drifts by using alternative methods for the data collection would provide further insight into the effect of adsorbate-free atoms reported here.

Conclusions

The comparison of experimentally obtained difference XANES fingerprints with theoretical difference XANES of model clusters (signatures) is a strategy for the characterization of coverage dependent adsorption sites. A single oxygen atom adsorbed on the Pt_6 Janin cluster modifies X-ray absorption properties of the adsorbate-free Pt atoms. It has been shown how the related electronic effects affect theoretical XANES spectra. Difference XANES calculated on a per atom basis reveal contribution of the adsorbate-free atoms to the averaged Δ-XANES response of the system. The resulting *all-atoms* signatures of the bridged, fcc, and hcp configurations are different from the corresponding *limited-adsorber* signatures currently used for surface adsorbate $\Delta\mu$ analysis. The most substantial difference is a negative contribution due to a positive shift of the absorption edge for the adsorbate-free atoms, which is related to the shift of the cluster Fermi level upon adsorption of oxygen. The presented results indicate that interpretation of Δ-XANES fingerprints is model dependent. It is expected that for a much larger, realistic electrochemical cluster the limited adsorber signatures more adequately represent the case of low adsorbate coverage. The experimentally observed negative contributions at higher coverages can be attributed to the influence of the adsorbate-free atoms. In addition, it is emphasized that the experimental Δ-XANES fingerprints are subject to an alignment error due to a shift of the energy scale in an experiment. The related uncertainty impedes discrimination of the fingerprints.

Acknowledgment. Thanks are due to David E. Ramaker, John J. Rehr, Carlo U. Segre, and Eugene S. Smotkin for helpful discussions.

Supporting Information Available: Figure 1S and Table 1S. This material is available free of charge via the Internet at http://pubs.acs.org.

References

(1) Iwasawa, Y. *X-ray Absorption Fine Structure for Catalysts and Surfaces*; World Scientific: Singapore, New Jersey, London, Hong Kong, 1996; Vol. 2, pp 3−6.

(2) McBreen, J.; Mukerjee, S. *J. Electrochem. Soc.* **1995**, *142*, 3399.

(3) Mathew, R.; Russell, A. *Top. Catal.* **2000**, *10*, 231.

(4) Roth, C.; Martz, N.; Buhrmester, T.; Scherer, J.; Fuess, H. *Phys. Chem. Chem. Phys.* **2002**, *4*, 3555.

(5) Allen, P. G.; Conradson, S. D.; Wilson, M. S.; Gottesfeld, S.; Raistrick, I. D.; Valerio, J.; Lovato, M. *J. Electroanal. Chem.* **1995**, *384*, 99.

(6) Stoupin, S.; Chung, E.-H.; Chattopadhyay, S.; Segre, C. U.; Smotkin, E. S. *J. Phys. Chem. B* **2006**, *110*, 9932.

(7) Stoupin, S.; Rivera, H.; Li, Z.; Segre, C. U.; Korzeniewski, C.; Casadonte, D. J., Jr.; Inoue, H.; Smotkin, E. S. *Phys. Chem. Chem. Phys.* **2008**, *10*, 6430.

(8) Teliska, M.; O'Grady, W. E.; Ramaker, D. E. *J. Phys. Chem. B* **2004**, *108*, 2333.

(9) Teliska, M.; O'Grady, W. E.; Ramaker, D. E. *J. Phys. Chem. B* **2005**, *109*, 8076.

(10) Roth, C.; Benker, N.; Buhrmester, T.; Mazurek, M.; Loster, M.; Fuess, H.; Koningsberger, D. C.; Ramaker, D. E. *J. Am. Chem. Soc.* **2005**, *127*, 14607.

(11) Teliska, M.; Murthi, V. S.; Mukerjee, S.; Ramaker, D. E. *J. Phys. Chem. C* **2007**, *111*, 9267.

(12) Scott, F. J.; Roth, C.; Ramaker, D. E. *J. Phys. Chem. C* **2007**, *111*, 11403.

(13) Scott, F. J.; Mukerjee, S.; Ramaker, D. E. *J. Electrochem. Soc.* **2007**, *154*, A396.

(14) Oudenhuijzen, M. K.; vanBokhoven, J. A.; Miller, J. T.; Ramaker, D. E.; Koningsberger, D. C. *J. Am. Chem. Soc.* **2005**, *127*, 1530.

(15) Janin, E.; von Schenck, H.; Göthelid, M.; Karlsson, U. O.; Svensson, M. *Phys. Rev. B* **2000**, *61*, 13144.

(16) Ankudinov, A. L.; Ravel, B.; Rehr, J. J.; Conradson, S. D. *Phys. Rev. B* **1998**, *58*, 7565.

(17) Ankudinov, A. L.; Nesvizhskii, A. I.; Rehr, J. J. *Phys. Rev. B* **2003**, *67*, 115120.

(18) Ankudinov, A. L.; Rehr, J. J.; Low, J.; Bare, S. R. *Phys. Rev. Lett.* **2001**, *86*, 1642.

(19) Bazin, D.; Sayers, D.; Rehr, J. J.; Mottet, C. *J. Phys. Chem. B* **1997**, *101*, 5332.

(20) Zabinsky, S. I.; Rehr, J. J.; Ankudinov, A.; Albers, R. C.; Eller, M. J. *Phys. Rev. B* **1995**, *52*, 2995.

(21) Rehr, J. J.; Ankudinov, A.; Zabinsky, S. I. *Catal. Today* **1998**, *39*, 263.

(22) Ankudinov, A. L.; Rehr, J. J.; Low, J. J.; Bare, S. R. *J. Chem. Phys.* **2002**, *116*, 1911.

(23) Ankudinov, A. L.; Rehr, J. J.; Low, J. J.; Bare, S. R. *Top. Catal.* **2002**, *18*, 3.

(24) von Barth, U.; Grossmann, G. *Solid State Commun.* **1979**, *32*, 645.

(25) Ravel, B.; Newville, M. *Phys. Scr.* **2005**, 1007.

(26) Ramaker, D. E.; Mojet, B. L.; Garriga Oostenbrink, M. T.; Miller, J. T.; Koningsberger, D. C. *Phys. Chem. Chem. Phys.* **1999**, *1*, 2293.

(27) Ramaker, D. E.; Teliska, M.; Zhang, Y.; Stakheev, A. Y.; Koningsberger, D. C. *Phys. Chem. Chem. Phys.* **2003**, *5*, 4492.

(28) Pascarelli, S.; Mathon, O.; Aquilanti, G. *J. Alloys Compd.* **2004**, *362*, 33.

(29) Pettifer, R. F.; Mathon, O.; Pascarelli, S.; Cooke, M. D.; Gibbs, M. R. J. *Nature (London)* **2005**, *435*, 78.

(30) Rose, A.; South, O.; Harvey, I.; Diaz-Moreno, S.; Owen, J. R.; Russell, A. E. *Phys. Chem. Chem. Phys.* **2005**, *7*, 366.

CT800544A